An Open-Source Self-navigated Multi-Echo Gradient Echo Acquisition for R_2* and QSM mapping using Pulseq and Model-Based Reconstruction

Xiaoqing Wang[1,2], Berkin Bilgic[1,2], Daniel Gallichan[3], Kwok-Shing Chan[4], and José P. Marques[4]
[1]*Massachusetts General Hospital, Athinoula A. Martinos Center for Biomedical Imaging, Charlestown, MA, United States,* [2]*Department of Radiology, Harvard Medical School, Boston, MA, United States,* [3]*Cardiff University Brain Research Imaging Centre, Cardiff, United Kingdom,* [4]*Donders Institute for Brain, Cognition and Behavior, Radboud University, Nijmegen, Netherlands*

Synopsis

We propose an open-source multi-echo GRE sequence and reconstruction algorithms for rapid acquisition and harmonization of QSM. This is implemented using Pulseq, where different sampling patterns are used across echoes to provide complementary information and facilitate the proposed MOdel BAsed (MOBA) reconstruction. MOBA estimates M0, R2* and frequency maps using nonlinear optimization and is implemented in BART to facilitate dissemination. B0 correction is performed using 1D navigators acquired during the crusher gradients in each repetition. Motion navigators inserted in the sequence permit robust estimation of motion parameters with time frames of ~13seconds, and will lend themselves to retrospective motion correction.

Introduction

There are various ongoing projects aiming at harmonization of protocols across vendors. In the context of QSM this has various levels: acquisition; computation of susceptibility maps and reporting. The currently recommended acquisition is a 3D multi-echo gradient echo (3DME-GRE) acquired axially to reduce acquisition time and be able to achieve 1 mm iso. resolution while using coils that might not be state of the art. In this scenario, an acquisition time of ~6 mins is required.

This remains long research or clinical applications (with motion being a risk), and does not account for respiration related B_0 fluctuations known to degrade R_2* and susceptibility maps. Furthermore it is never possible to know how similar the implementations are between different vendors e.g. in terms of gradient/RF spoiling, excitation profiles and image reconstruction.

We introduce a framework for acquisition based on Pulseq (1) that is vendor neutral and open source, and where data of subject motion and B_0 fluctuations are encoded for artifact reduction, and with an acquisition pattern that is compatible with model-based reconstruction to reduce scan time.

Methods

Pulseq was used to implement a 3DME-GRE sequence using controlled aliasing patterns that are shifted across-echo times (Fig.1a/b). A 1D navigator was added as part of the crusher to record (Fig.1a) respiration related information.
Acquisitions were performed on a 3T Prisma system equipped with a 32-channel coil using the following:

R=9-fold acceleration: $TR = 35ms$; $TE_1/\Delta TE/TE_6 = 3/5/28ms$; $\theta = 15^o$; acceleration $[R_y, R_z, Caipi_{z-shift}, Caipi_{z-echo-shift}] = [1, 9, 3, 2]$; Sagittal acquisition FOV=[256,198,225]mm, 1mm isotropic; Central [27 ,36] PEy and PEz lines were fully sampled and used for motion correction; acquisition time 4mins

R=12-fold acceleration: $[R_y, R_z, Caipi_{z-shift}, Caipi_{z-echo-shift}] = [1, 12, 4, 2]$; acquisition time 3mins, other parameters were kept the same.
One subject was scanned twice with the above protocol: either breathing normally or taking deep breaths to induce motion.

B_0 correction was implemented by fitting a first order polynomial to the phase of the FFT of the navigator data (in regions of sufficient SNR), and applying that correction across all echo readouts.

The use of navigators for motion correction was evaluated by reconstructing using various sliding windows (Fig.1c), and inspecting the motion correction parameters stability derived by mcflirt (fsl.fmrib.ox.ac.uk). To stabilize the reconstruction and make use of the expected signal model $S_0(r)e^{-TE_n(R_2^*-i2\pi\cdot f_{B0})}$, the fully sampled center of k-space was used as a reference/target 4D image, $S_{GT}(TE_{1->N})$. The multi-echo navigators, $S_{nav_n}(TE_{1->N})$, were reconstructed in an iterative SENSE framework with an L2 regularization on $\frac{\partial S_{GT}(TE_{N->1})}{\partial TE} - \frac{\partial S_{nav_n}(TE_{N->1})}{\partial TE}$.

MOdel-BAsed Reconstruction (MOBA): Different CAIPI patterns across the echoes and GRE signal modeling were exploited by solving (2):

$$x = (S_0, R_2^*, f_{B0})^T = \text{argmin}_x \sum_{\text{TE}} \|P\mathcal{F}C \cdot S_0 \cdot \text{e}^{-\text{TE}\cdot R_2^* + i2\pi\cdot\text{TE}\cdot f_{B0}} - Y\|_2^2 + R(x)$$

While a joint L1-Wavelet sparsity constraint was applied to S_0 and R_2* maps, Sobolev regularization was adopted for f_{B0} to enforce smoothness. MOBA was implemented on BART (3) and used GPU acceleration.
Sequence/reconstruction code/data:
https://anonymous.4open.science/r/pulseq_qsm-2DF5

Results

Fig.2a shows that the B_0 navigation can clearly detect respiration fluctuations, with the required correction being greater on lower coils, as well as introducing a correction that has an impact on the latter echo and R_2* maps.
Fig.3 depicts R2*, M0 and QSM estimates obtained using SENSE at R=9 and R=12-fold acceleration. SEPIA's (4) implementation of LP-CNN (5) was used for

dipole inversion. MPPCA (6) was applied on multi-echo SENSE volumes for denoising.
Fig.4 shows the quality of motion estimates in the deep-breathing acquisition as a function of temporal resolution and regularization. Fidelity of the motion estimates is reduced at the temporal resolution of 8.8 sec, whereas better estimates were obtained by increasing the sliding-windowing factor at the cost of increasing the motion sensitivity to 13.2 sec.
Fig.5 shows two slices from MOBA and SENSE reconstructions at R=9. Improved SNR is observed in the R_2* and M_0 maps, yet artifacts were visible in the lower slice. Tissue phase was obtained using V-SHARP directly on the f_{B0} estimate.

Discussion/Conclusion

Proposed framework can be used to benchmark the quality of existing sequences and understand the impact of motion/respiration in manufacturer protocols. R_2* mapping quality is typically plagued by short TEs used (as was the case in this pilot data), the use of B_0 navigation allows longer TEs, while MOBA combined with controlled aliased patterns across echos allows higher acceleration, keeping clinically acceptable acquisition times in systems with poorer gradients and number of coils. Future work will focus on retrospective motion correction using the navigators.
Fig.4 shows that a 3 min acquisition at R=12 is feasible, and no artifacts were visible. Regardless, g-factor penalty contributed to the increased noise especially in the middle of the FOV, which can be mitigated using e.g. wave-CAIPI (7). As pointed out by the arrows in Fig.5, there are residual fat and B0-related artifacts in the lower slices in the MOBA reconstruction. These can be addressed by modeling the fat component in the signal model (2). Future work will explore the ability to accelerate acquisitions in more standard clinical RF setups with 12 and 16 channels using wave encoding and water-fat separated MOBA reconstruction.

Acknowledgements

This work was supported by research grants NIH R01 EB032378, R01 EB028797, R03 EB031175, U01 EB025162, P41 EB030006, U01 EB026996, the NWO grant FOM-N-31/16PR1056, and the NVidia Corporation for computing support.

References

1. Layton KJ, Kroboth S, Jia F, et al. Pulseq: A rapid and hardware-independent pulse sequence prototyping framework. Magn. Reson. Med. 2017;77:1544–1552.

2. Tan Z, Unterberg-Buchwald C, Blumenthal M, et al. Free-Breathing Liver Fat, R_2^* and B_0 Field Mapping Using Multi-Echo Radial FLASH and Regularized Model-based Reconstruction. 2021 doi: 10.48550/arXiv.2101.02788.

3. Uecker M, Tamir JI, Ong F, Lustig M. The BART toolbox for computational Magnetic Resonance Imaging. http://wwwuser.gwdg.de/~muecker1/basp-uecker2.pdf. Accessed November 8, 2022.

4. Chan K-S, Marques JP. SEPIA—Susceptibility mapping pipeline tool for phase images. Neuroimage 2021;227:117611.

5. Lai K-W, Aggarwal M, van Zijl P, Li X, Sulam J. Learned Proximal Networks for Quantitative Susceptibility Mapping. Med. Image Comput. Comput. Assist. Interv. 2020;12262:125–135.

6. Veraart J, Novikov DS, Christiaens D, Ades-Aron B, Sijbers J, Fieremans E. Denoising of diffusion MRI using random matrix theory. Neuroimage 2016;142:394–406.

7. Bilgic B, Gagoski BA, Cauley SF, et al. Wave-CAIPI for highly accelerated 3D imaging. Magn. Reson. Med. 2015;73:2152–2162.

Figures

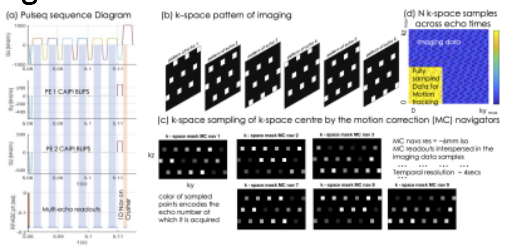

Fig.1 (a) One TR of the 3D-MEGRE sequence implemented in pulseq with the readouts and B_0 navigation identified in blue and red respectively. Two types of readouts coexist: "imaging" and "motion correction"; b) shows imaging k-space mask for an acceleration factor $[R_y, R_z, CAIPI_z] = [1, 9, 3]$, with this pattern being shifted across echos $[Echoy_{shift}, Echoz_{shift}] = [0, 2]$; c) shows k-space mask of successive Motion navigators (54 navs are acquired); d) in this form most k-space coordinates are acquired (6/9 in imaging are, and fully or over sampled in k-space centre)

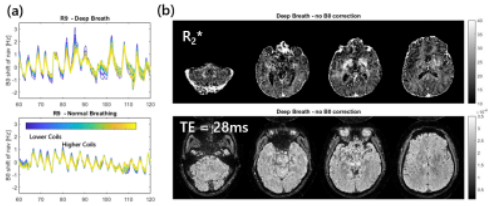

Fig.2 Plot of B_0 shift measured per receiver coil as a function of time [s] for two acquisitions with normal and deep breathing. The color of each line encoded the position in the Head-Foot direction of maximum sensitivity of an RF coil. Time courses were temporally smoothed and show that signal in lower coils (in blue) is more affected by B_0 respiration drifts. (b) shows the last echo images and R_2* maps (computed with ARLO) of four representative slices.

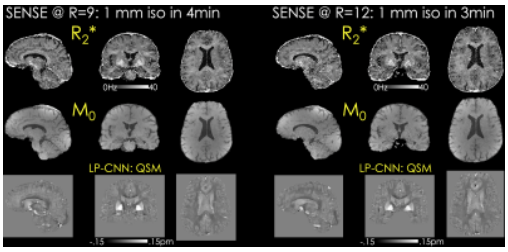

Fig.3 R_2*, M_0 and susceptibility maps obtained from R=9 (left) and R=12-fold (right) accelerated Pulseq acquisitions reconstructed using SENSE. Multi-echo SENSE volumes were denoised using MPPCA prior to parameter mapping. SEPIA's implementation of LP-CNN dipole inversion permitted high-quality QSM reconstructions from these 4 min (R=9) and 3 min (R=12) acquisitions at 1 mm isotropic resolution. B_0 correction was performed on each volume to remove 0th order phase fluctuations across TRs.

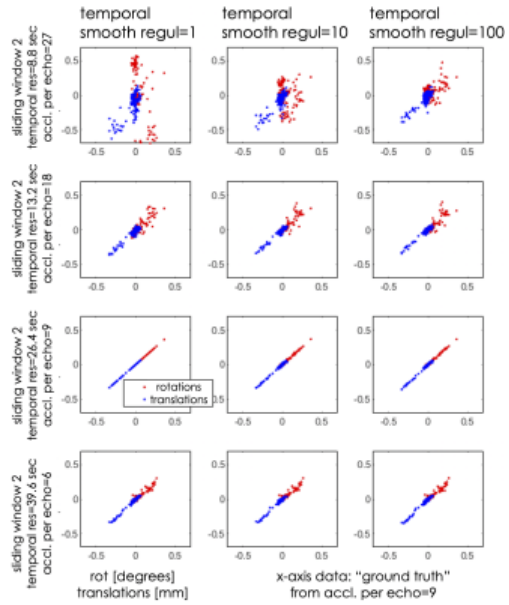

Fig.4 Each plot is a scatter plot of the motion regressors (x,y,z rotations and translations in red and blue) derived from a given reconstruction (in y) vs the “ground truth reconstruction (in x), based on an effective acceleration factor per echo of 9 - which results in good quality reconstructions for the whole brain data). Different columns represent increasing regularization of the individual reconstruction and rows represent varying temporal resolution of the MC navigators.

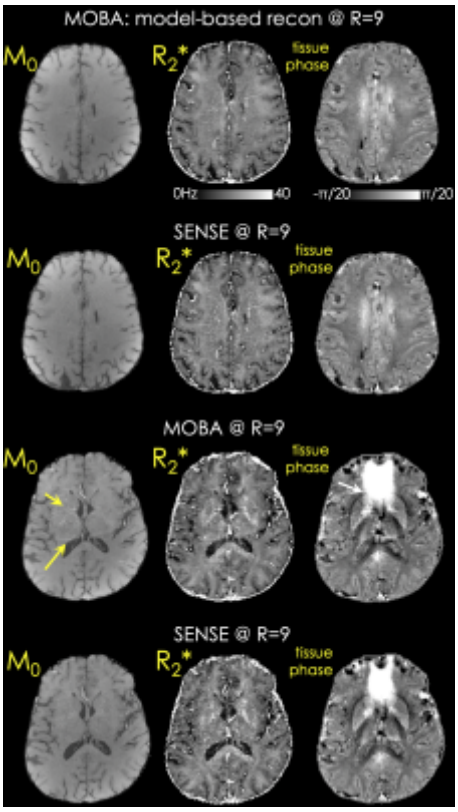

Fig.5 First and second rows compare M0, R2* and tissue phase maps obtained from the proposed MOBA and standard SENSE reconstructions. Model-based regularized reconstruction in MOBA helps boost SNR in the reconstructed maps. Third and fourth rows compare the two reconstruction strategies on a lower slice, where field homogeneity is poorer. In this case fat signal (yellow arrows) and B0 inhomogeneity (white arrow) lead to artifacts in MOBA. Incorporating water-fat modeling into MOBA and replacing the Sobolev regularization on the field map are expected to improve the image quality.